

Realization of negative permittivity of Co_2Z hexagonal ferrite and left-handed property of ferrite composite material

To cite this article: Fang Xu *et al* 2009 *J. Phys. D: Appl. Phys.* **42** 025403

View the [article online](#) for updates and enhancements.

You may also like

- [Electrochemical Characterization of \$\text{TiO}_2\$ Films Formed by Cathodic EPD in Aqueous Media](#)
Próspero Acevedo-Peña, Gerardo Vázquez, Dionisio Laverde *et al.*
- [Semiconductive Behavior of Anodic Titanium Oxide Films with Different Thicknesses](#)
Eri Fujimura, Yuhei Fujioka, Hiroaki Tsuchiya *et al.*
- [The Effect of the Semiconductive Screen on Space Charge Suppression in Cross-Linked Polyethylene](#)
Lin Li, , Bai Han *et al.*

ECS
The
Electrochemical
Society
Advancing solid state &
electrochemical science & technology

DISCOVER
how sustainability
intersects with
electrochemistry & solid
state science research

Realization of negative permittivity of Co_2Z hexagonal ferrite and left-handed property of ferrite composite material

Fang Xu¹, Yang Bai¹, Lijie Qiao¹, Hongjie Zhao² and Ji Zhou²

¹ Corrosion and Protection Center, Key Laboratory of Environmental Fracture (Ministry of Education), University of Science and Technology Beijing, Beijing 100083, People's Republic of China

² State Key Laboratory of New Ceramics and Fine Processing, Tsinghua University, Beijing 100084, People's Republic of China

E-mail: baiy@mater.ustb.edu.cn and lqiao@ustb.edu.cn

Received 16 July 2008, in final form 7 October 2008

Published 18 December 2008

Online at stacks.iop.org/JPhysD/42/025403

Abstract

The complex permeability and complex permittivity of Co_2Z hexagonal ferrite and the microwave properties of ferrite composite material consisting of Co_2Z and yttrium iron garnet (YIG) slabs have been discussed in this paper. Negative permittivity is obtained in the semiconductive Co_2Z , and Zn doping can further enhance the dielectric resonance. However, the high conductivity prevents Co_2Z from producing negative permeability that originates from ferromagnetic resonance, i.e. double negative properties cannot be obtained in semiconductive or metallic ferromagnet. When Co_2Z is combined with YIG, the composite structure shows magneto-tunable left-handed properties where Co_2Z provides negative permittivity and YIG provides negative permeability.

(Some figures in this article are in colour only in the electronic version)

1. Introduction

Left-handed materials (LHMs) that are of negative permittivity and negative permeability simultaneously have attracted considerable attention due to their exotic physical properties and potential applications in optical and microwave devices [1–6]. Since the first LHM consisting of split-ring resonators (SRRs) and metallic rods was made in 2000, similar artificial structures have been well developed and optimized [7–13]. However, their left-handed properties originate from the structure rather than deriving directly from the materials' nature; thus it becomes a challenging and interesting subject to realize left-handed properties using the materials' intrinsic properties. In recent years, some LHMs based on continuous media, such as ferrites and ferroelectric ceramics, were studied in theory and made in experiment [14–19]. In the LHMs composed of ferrites, ferrites were used to produce negative permeability through the ferromagnetic resonance (FMR) and were combined with metallic wires with negative permittivity [16, 17].

Ferrites are a type of magnetic media with complex permeability and complex permittivity simultaneously, whose dielectric properties are closely associated with the conduction mechanism. It was reported that ferrites could become semiconductors and exhibit negative permittivity after special processing [20]. It seems possible to produce both negative permeability and negative permittivity in a ferrite.

Co_2Z hexagonal ferrite was selected as the candidate because its permeability turns negative above 2 GHz due to spin resonance [21, 22] and its high conductivity might induce negative permittivity [20]. In this paper, we studied the magnetic and dielectric properties of Co_2Z , as well as the microwave characters of the ferrite composite material consisting of Co_2Z and yttrium iron garnet (YIG). The left-handed properties were obtained in the composite, where Co_2Z provided negative permittivity and YIG provided negative permeability around its FMR frequency. Moreover, the possibility of realizing a single phase LHM using a semiconductive ferromagnet is discussed.

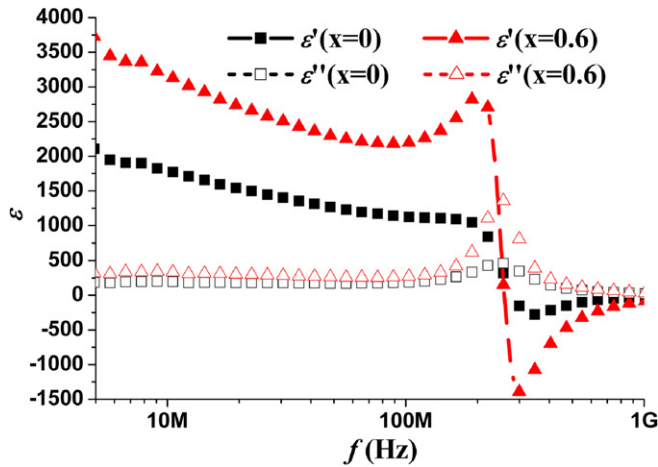


Figure 1. Complex permittivity for the sample of $\text{Ba}_2\text{Co}_2\text{Fe}_{24-x}\text{Zn}_x\text{O}_{41}$ ($x = 0, x = 0.6$).

2. Experimental

Co_2Z hexagonal ferrite with a composition of $\text{Ba}_3\text{Co}_2\text{Fe}_{24-x}\text{Zn}_x\text{O}_{41}$ ($x = 0, 0.6$) was prepared using the conventional ceramics method. After calcination at 1290°C , single phase Co_2Z powder was obtained, which is confirmed by means of powder x-ray diffraction. The dry-pressed rings, pellets and slabs were sintered at 1300°C for 6 h. The sintered slabs were sliced and ground precisely to the required dimensions. The YIG slab is commercially available. The frequency dependences of permeability and permittivity were measured using an Agilent 4991A impedance/material analyzer from 1 MHz to 1 GHz. The microwave properties of the samples were measured in a rectangular waveguide (WR284, $a = 72.14$ mm and $b = 34.04$ mm). The slab samples filled the cross section of the waveguide. The S parameters were measured by an HP 8720ES network analyzer. The composite sample consisted of a Co_2Z slab and a YIG slab and there was a gap (d) between them. An electromagnet was used to generate the external magnetic field (H_0) and the magnetic field was perpendicular to the propagation direction of electromagnetic waves.

3. Results and discussion

Figure 1 shows the complex permittivity for the samples ($x = 0, 0.6$) sintered at 1300°C . The dielectric spectra show typical frequency-dispersive character and a resonance peak appears at about 200 MHz. The dielectric permittivity turns negative above the resonance frequency.

The sample with Zn substitution ($x = 0.6$) has higher permittivity and stronger resonance. In the lattice of Z-type hexaferrite, the transition metal ions, such as Fe^{3+} , Fe^{2+} , Co^{2+} , Co^{3+} and Zn^{2+} , are located at the interstitial sites. The loss of oxygen during the sintering process results in the valency variation of transition metal ions and the formation of charge carriers (n-type and p-type). If the ferrite were to be sintered at high temperature and not annealed in oxygen, the specimens would be semiconductive. The high electric conductivity of the semiconductor makes it just like a metal

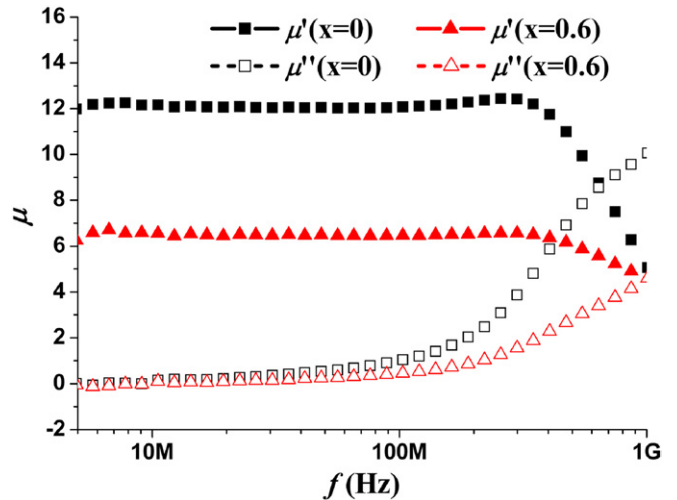


Figure 2. Complex permeability for the sample of $\text{Ba}_2\text{Co}_2\text{Fe}_{24-x}\text{Zn}_x\text{O}_{41}$ ($x = 0, x = 0.6$).

in many aspects and the oscillation of electrons results in negative permeability. Similarly, it was reported that some organic semiconductors exhibited negative capacitance in the impedance measurement [23].

Moreover, the active energy of electronic transfer between Fe^{3+} and Fe^{2+} is low, the electronic transfer between Fe^{3+} and Fe^{2+} in octahedral sites gives the main contribution to the electric conduction mechanism of ferrite [24–28]. Zn^{2+} ions prefer to occupy tetrahedral sites and drive some Fe^{3+} to octahedral sites, which contribute to the increment in electric conductivity. The dielectric permittivity of ferrites is directly proportional to the root mean square of the conductivity $\epsilon \propto (1/\rho)^{1/2}$ [29]. Zn substituted Co_2Z ($x = 0.6$) exhibits higher dielectric permittivity and stronger dielectric resonance.

Figure 2 shows the complex permeability of the samples. Both the samples have relaxation dispersion and the Zn doping induces a drop in permeability. The permeability is proportional to M_s^2 and is inversely proportional to magnetocrystalline anisotropy (K_1). Nonmagnetic Zn^{2+} ions prefer to occupy the tetrahedral sites antiparallel to the whole magnetic moment, so the saturation magnetization increases with Zn doping. However, since the introduction of nonmagnetic Zn^{2+} ions can decrease the Curie temperature, room-temperature (RT) saturation magnetization decreases. It was reported that the RT saturation magnetization drops when the Zn content is higher than 0.5 in Co_2Z [30]. In addition, the substitution of Zn in Co_2Z does not change K_1 apparently [31]. Hence, the permeability decreases in the Zn-doped Co_2Z .

According to classic ferromagnetism, the permeability turns negative above the FMR frequency with the aid of the bias magnetic field. For hexagonal ferrites, the strong magnetocrystalline field in the oriented sample may play the role of a bias field instead of an external field. It was reported that negative permeability was obtained above 2 GHz in the oriented Co_2Z sample [21, 22]. However, we did not use the oriented sample and the bias field was not applied in the impedance measurement, so there was no negative permeability in figure 2.

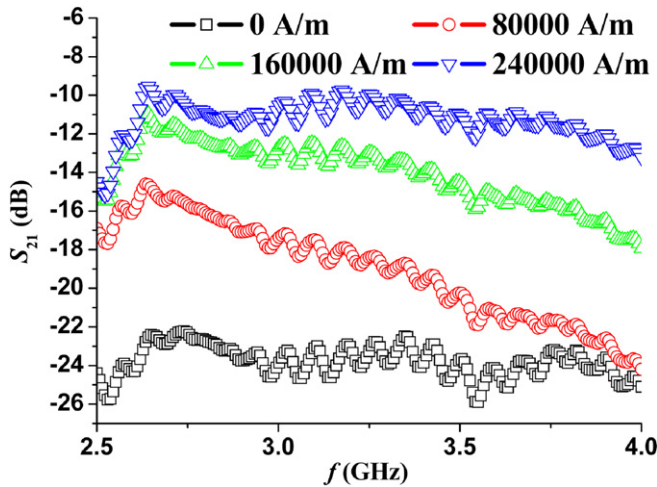


Figure 3. Transmission spectra for $\text{Ba}_2\text{Co}_2\text{Fe}_{23.4}\text{Zn}_{0.6}\text{O}_{41}$ measured under different magnetic fields.

The microwave properties of Zn doped Co_2Z ($x = 0.6$) under an external magnetic field were measured using the waveguide method, and the results are shown in figure 3. According to Maxwell equations, the microwave cannot propagate in single negative medium (negative permeability or negative permittivity), therefore a forbidden band appears; the microwave can propagate in double negative medium, so a passband appears. In the transmission spectra, the absence of a tunable passband indicates that Co_2Z does not possess negative permeability and negative permittivity simultaneously. In addition, there is also no obvious tunable forbidden band, which is the evidence of negative permeability around FMR frequency. It is presumed that the high conductivity of the sample may prevent FMR.

Then we simulated the transmission properties of ferrites with different conductivities at FMR using the method of finite difference time domain and perfect boundary approximation. In the simulation, a gyromagnetic slab was filled in a rectangle space with a cross section of $72 \times 34 \text{ mm}^2$ where a transverse electric wave was excited and two ports were far away from the sample. The boundaries of the calculated space were set as perfect electric walls and perfect magnetic walls. Figure 4 shows the simulated transmission spectra of ferrite slabs with different conductivities. The results show that the forbidden band corresponding to FMR appears when the conductivity of the sample is relatively low. When the conductivity increases, the narrow forbidden band disappears gradually and a very broad forbidden band appears instead, which may originate from the plasma resonance of the semiconductive sample. The results indicate that the high conduction of the sample destroys the FMR; therefore negative permeability and negative permittivity cannot be produced simultaneously using a metallic or semiconductive ferromagnet.

To confirm the negative permittivity of Co_2Z and achieve LHM, we combined the Co_2Z ($x = 0.6$) slab with the YIG slab and measured the transmission properties. Figure 5(a) shows the transmission spectra of a single YIG slab under different magnetic fields. The YIG slab can produce negative permeability around the FMR frequency, so a magneto-tunable forbidden band is observed. The frequency of the

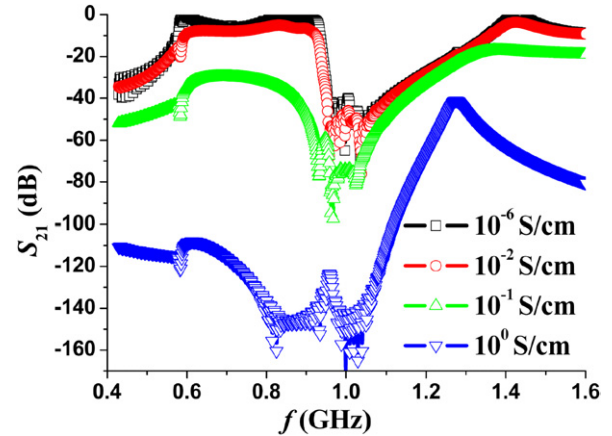


Figure 4. Simulated transmission spectra for ferrites with different conductivities under a 240000 A m^{-1} bias magnetic field.

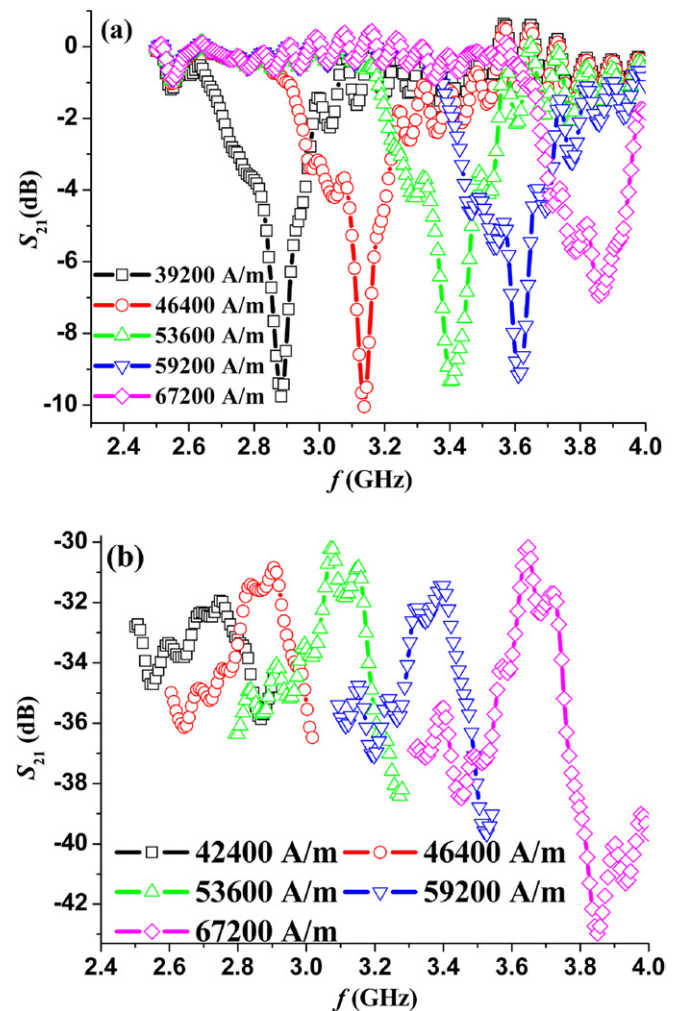


Figure 5. (a) Amplitude of S_{21} for the YIG slab measured under different magnetic fields. (b) Amplitude of S_{21} for the composite ($d = 3 \text{ mm}$) measured under different bias magnetic fields.

downward peak rises from 2.9 to 3.9 GHz when the magnetic field increases from 39200 to 67200 A m^{-1} . The measured transmission spectra of the composite structures are shown in figure 5(b). In the composite, a Zn doped Co_2Z ($x = 0.6$) slab ($72 \times 34 \times 5 \text{ mm}^3$) and a YIG slab ($72 \times 34 \times 1 \text{ mm}^3$) are

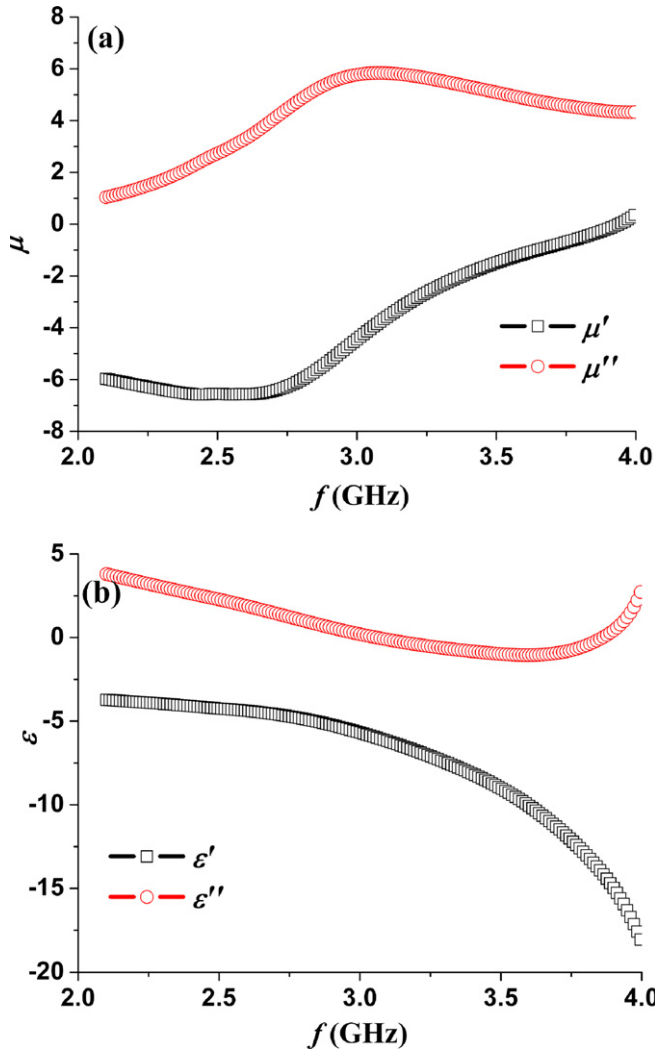


Figure 6. Retrieved frequency dependence of effective permeability (a) and effective permittivity (b) based on the calculated scattering parameters. (') and (") denote the real and the imaginary parts of the parameters, respectively.

placed parallelly with a gap $d = 3$ mm and fill the section of the waveguide. An upward peak, instead of a downward peak, appears in the transmission spectra. The centre frequency of the transmission peak shifts from 2.7 to 3.7 GHz, while the bias magnetic field increases from 42 400 to 67 200 A m^{-1} . The frequency of the upward peak corresponds to that of the downward peak for YIG under the same field condition. The transmission passband results from the coexistence of negative permeability and negative permittivity in the composite. The properties of the ferrite composite are the same as that of the left-handed composite consisting of YIG and metallic wires, where YIG provides negative permeability and metallic wires provide negative permittivity [16, 17]. In our ferrite composite, Co_2Z takes the place of metallic wires to provide negative permittivity.

The effective permeability and negative permittivity of the composite were retrieved using the simulated scattering parameters [33–36]. All the simulated conditions are in complete accordance with practice. Both Co_2Z and YIG

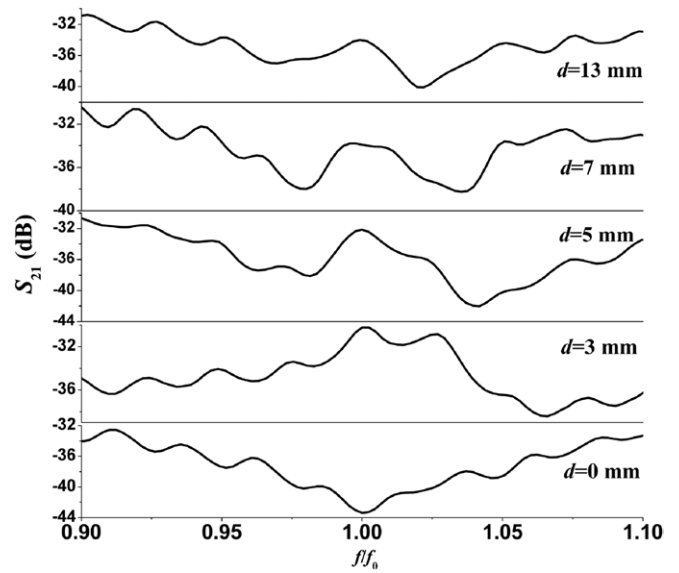


Figure 7. Amplitude of S_{21} for the sample with different thicknesses d measured under a 53 600 A m^{-1} bias magnetic field.

were considered as gyromagnetic media. Co_2Z was set as a semiconductor with a conductivity of 1 S m^{-1} and YIG was set as an isolator. The distance between the two slabs is 1 mm. Figure 6 shows that both effective permeability and permittivity are negative. The calculated results support the experimental results about the left-handed properties of the composite consisting of Co_2Z and YIG slabs.

In the composite of YIG and metallic wires, the electromagnetic interaction between YIG and metallic wires destroys the left-handed properties; therefore a gap between them is needed [15–17, 32]. The condition is similar to our ferrite composite, and the effect of the gap (d) between the YIG slab and the Co_2Z slab on the left-handed property is also discussed. The transmission spectra of the ferrite composite with different d measured under a bias field of 53 600 A m^{-1} are shown in figure 7. When d is 0 mm, the left-handed property is prevented due to the negative influence of the electromagnetic interaction and an apparent forbidden band appears. When d is 3, 5, 7 or 13 mm, an obvious transmission passband is observed in the transmission curves because the negative effect of electromagnetic interference is reduced. On the other hand, the width of the passband decreases and the loss increases with the rise in d and the transmission passband disappears when d is large enough.

4. Conclusion

In summary, the complex permeability and complex permittivity of Co_2Z and microwave properties of the composite consisting of Co_2Z and YIG slabs have been discussed. High temperature sintered Co_2Z is semiconductive and produces negative permittivity above the dielectric resonance frequency. Zn doping can enhance the dielectric resonance of Co_2Z further. But the high conductivity prevents Co_2Z from producing negative permeability. When Co_2Z is combined with YIG, the composite structure shows magnetotunable left-handed properties where Co_2Z provides negative

permittivity and YIG provides negative permeability. It is a real LHM whose negative parameters both inherit from the materials' nature. Although LHM was not made in a single phase material, this composite material can significantly promote the development of LHM based on continuous media. If a special process can make one part of the ferromagnet semiconductive and the other insulated, LHM may be realized in one medium.

Acknowledgments

This work was supported by the National Science Foundation of China under grants of 50702005, by the Specialized Research Fund for the Doctoral Program of Higher Education of 20070008027, by the Program for Changjiang Scholars and Innovative Research Team in University under grant of IRT0509 and by the Beijing Municipal Commission of Education under grant of SYS100080419.

References

- [1] Pendry J B 2000 *Phys. Rev. Lett.* **85** 3966
- [2] Lim S, Caloz C and Itoh T 2004 *IEEE Microw. Wirel. Co.* **14** 277
- [3] Veselago V G 1968 *Sov. Phys.—Usp.* **10** 509
- [4] Pendry J B, Schurig D and Smith D R 2006 *Science* **312** 1780
- [5] Tassin P, Sahyoun X and Veretennicoff I 2008 *Appl. Phys. Lett.* **92** 203111
- [6] Rahm M, Schurig D, Roberts D A, Cummer S A, Smith D R and Pendry J B 2008 *Photon. Nanostruct.: Fundam. Appl.* **6** 87
- [7] Smith D R, Padilla W J, Vier D C, Nemat-Nasser S C and Schultz S 2000 *Phys. Rev. Lett.* **84** 4184
- [8] Marques R, Medina F and Rafi-El-Idrissi R 2002 *Phys. Rev. B* **65** 144440
- [9] Baena J D, Marques R and Medina F 2004 *Phys. Rev. B* **69** 014402
- [10] Gay-Balmaz P and Martin O J F 2002 *Appl. Phys. Lett.* **81** 939
- [11] Ran L, Huangfu J, Chen H, Li Y, Zhang X M, Chen K and Kong J A 2004 *Phys. Rev. B* **70** 073102
- [12] Chen H, Ran L, Huangfu J, Zhang X M, Chen K and Grzegorzczuk T M and Kong J A 2004 *Phys. Rev. E* **70** 057605
- [13] Chen H, Ran L, Huangfu J, Zhang X, Chen K, Grzegorzczuk T M and Kong J A 2004 *J. Appl. Phys.* **96** 5338
- [14] Pimenov A, Loidl A, Przyslupski P and Dabrowski B 2005 *Phys. Rev. Lett.* **95** 247009
- [15] Rachford F J, Armstead D N, Harris V G and Vittoria C 2007 *Phys. Rev. Lett.* **99** 057202
- [16] He Y X, He P, Yoon S D, Parimi P V, Rachford F J, Harris V G and Vittoria C 2007 *J. Magn. Magn. Mater.* **313** 187
- [17] Zhao H J, Zhou J, Zhao Q, Li B, Kang L and Bai Y 2007 *Appl. Phys. Lett.* **91** 131107
- [18] Bai Y, Chen H, Zhang J, Luo Y, Li B, Ran L, Kong J and Zhou J 2007 *Opt. Express* **15** 8284
- [19] Wu R X, Zhang X K, Lin Z F, Chui S T and Xiao J Q 2004 *J. Magn. Magn. Mater.* **271** 180
- [20] Zhang H G, Zhou J, Yue Z X, Wu P G, Gui Z L and Li L T 2000 *Mater. Lett.* **43** 62
- [21] Allegri P, Autissier D and Taffary T 1997 *Key Eng. Mater.* **132–136** 1424
- [22] Liao S B 2000 *Ferromagnetism* (Beijing: Science Press) p 65 chapter 12
- [23] Ehrenfreund E, Lungenschmied C, Dennler G, Neugebauer H and Sariciftci N S 2007 *Appl. Phys. Lett.* **91** 012112
- [24] Purushotham Y and Reddy P V 1996 *Int. J. Mod. Phys. B* **10** 319
- [25] Abo A M, Ata E and Ahmed M A 2000 *J. Magn. Magn. Mater.* **208** 27
- [26] Rezlescu N and Rezlescu E 1974 *Solid State Commun.* **14** 69
- [27] Ismael H, El-Nimr M K, Abou El Ata A M, El Hiti M A, Ahmed M A and Murakhowskii A A 1995 *J. Magn. Magn. Mater.* **150** 403
- [28] Ahmed M A, El-Nimr M K, Tawfik A and Aboelata A M 1989 *Phys. Status Solidi a* **114** 377
- [29] Koops C G 1951 *Phys. Rev.* **83** 121
- [30] Zhang H G, Zhou J, Wang Y L, Li L T, Yue Z X and Gui Z L 2002 *Ceram. Int.* **28** 917
- [31] Wang X H, Li L T, Yue Z X, Su S Y, Gui Z L and Zhou J 2002 *J. Magn. Magn. Mater.* **246** 434
- [32] Dewar G 2005 *J. Appl. Phys.* **97** 10Q101
- [33] Chen X D, Grzegorzczuk T M, Wu B I, Pacheco J and Kong J A 2004 *Phys. Rev. E* **70** 016608
- [34] Zhao Q, Kang L, Du B, Zhao H J, Xie Q, Huang X, Li B, Zhou J and Li L 2008 *Phys. Rev. Lett.* **101** 027402
- [35] Koschny T, Markos P, Smith D R and Soukoulis C M 2003 *Phys. Rev. E* **68** 065602
- [36] Smith D R, Schultz S, Markos P and Soukoulis C M 2002 *Phys. Rev. B* **65** 195104